503

Relationship between block shape and street network integration

ERMAL SHPUZA,

KENNESAW STATE UNIVERSITY, MARIETTA, USA

_____

ABSTRACT

The paper inquires into the link between geometric and topological characteristics of street networks by studying the shape of urban blocks, which are considered as spatial remainders to the street network. Block shapes in a sample of seventy cities are analyzed based on the two coupled measures of shape elongation and fragmentation. The distribution of datapoints in the scatterplot between block shape elongation and fragmentation reveals a distinct two-tail distribution with a heavy tip, which indicates the prevalence of three types of blocks: compact and convex, elongated and convex, and internally dissected through cul-de-sacs streets, where blocks with both overly stretched and bent shapes are infrequent, thus producing a rarified region between the two tails. To quantify the variance in the distribution of block shape in the scatterplots among the cities, a shape configuration matrix is proposed based on the ratios of the amount elongation and fragmentation within the two tails to the rest of the scatterplot. The combined ratios in the two tails show a considerable correlation with the global street network integration, which is further increased when taken together with the local measure of axial line connectivity. The proposed measures and the classification method shed light on the link between geometric and topological characteristics of street networks, support comparative studies, and reveal principles of urban form synthesis applicable to urban modeling, planning and design.

KEYWORDS

Urban block, street network, shape description, block shape configuration

1   INTRODUCTION

An important issue related to the space syntax description of cities involves the understanding of the distinct roles the foreground arterials and background neighbourhood streets play in structuring the spatial qualities of street networks (Hillier et al. 2010). The arterials originate

from the intercity road systems that connect settlements with each other or emerge as boulevards introduced through planned interventions. The effect of foreground arterials on the syntactic structure is easier to grasp, longer arterials lead to more integrated street networks (Figueiredo and Amorim, 2005; Shpuza, 2013), and simpler foreground structures create more spatial cohesion. Large-scale planning interventions throughout history have employed the opening of long boulevards to improve the accessibility to remote areas in cities. Meanwhile, the effect of background streets on the global spatial structure is equally as important. Urban design and planning projects also operate at the local scale in the areas between main arterials, while street patterns are affected by local-scale decisions of land subdivision as related to plot and block requirements and cultural influences.

While we do have models of describing street patterns in terms of their geometry and topology (Marshall, 2005), the effect of background streets on the overall syntactic structure is less understood, in part because of the unknown effect of cropping and analyzing separate patches of streets on the overall global syntactic measures. In recent years, several studies in space syntax have sought to understand the link between geometric characteristics, such as metric length and angle, on topological features of street networks, while focusing on the street network itself (Hillier, 1999; Hillier et al., 2010; Peponis et al., 2008; Serra and Hillier, 2019; Turner, 2001).
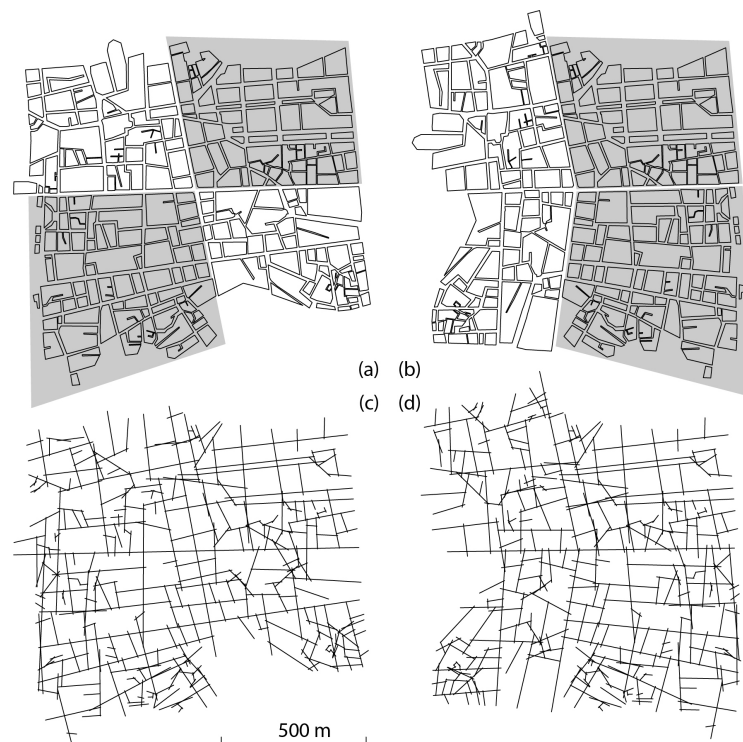

(a) (b)
(c) (d)

500 m

Figure 1: Four quadrants in Catania (a), rearranged (b) using identical urban blocks produce a different street network as indicated by changes in the axial map structure (c, d).

While we cannot easily account for the effect of separate patches of street networks on the global spatial structure, we can describe and measure the shape of urban blocks as single entities

separate from the bounding background network streets. The link between street patterns and block shape is quite evident (Southworth and Owens, 1993): gridiron patterns produce rectangular blocks, distributory patterns produce large blocks dissected by internal dendritic and cul-de-sac streets, while conjoint patterns produce a combination of rectangular and L-shape blocks. Given that blocks are intra-cells of the street network or spatial remainders to them in Euclidian space, they can have a direct link with the street network topology. Thus, the study advances the proposition that, notwithstanding the effect of the foreground network on the global topology of the street network, topo-geometric properties of blocks have a measurable relationship with the global integration of street networks. At first, this conjecture can be easily refuted since reshuffling the same set of blocks can produce different street arrangements. For example, four sectors in Catania, Italy are rotated and flipped to produce a different street network while maintaining the same blocks (Figure 1). However, we should also note that the reshuffling of blocks has produced an unintelligible street network with several T-junctions where lines of movement are discontinued (Figure 1(b, d)), as indicated by the reduction of mean integration from 1.564 to 1.432, the intelligibility (R^2 in plot C vs I) from 0.424 to 0.289, and a slight change of the mean connectivity from 4.02 to 3.93. Given that street networks in cities evolve by prioritizing the continuity lines (Amorim and Figueiredo, 2005) and facilitating through-movement (Hillier et al., 1993), it is possible to reassess the original hypothesis that blocks shapes are not only directly related to the immediate bounding street patterns, but also have an affinity with the topological structure of the street network in the global scale.

2   AXIAL MAPS AND AXIAL BLOCKS

The study uses the dataset of axial maps (Hillier and Hanson, 1984) of 70 towns and cities on the Adriatic and Ionian coasts of Greece, Albania, Montenegro, Croatia, Slovenia, and Italy (Shpuza, 2014; Shpuza, 2017), hereafter referred to as "AI" (Table 1). First, axial maps are studied according to space syntax measures of connectivity and topological depth, and second, according to the shape of axial blocks, which are defined as polygons surrounded by axial lines on all sides. Blocks are generated by subtracting from the urban area axial lines that are made two-dimensional using a small width of about 0.2 m. While this gives a high fidelity of axial blocks to the base axial map, it also has the disadvantage of producing many small polygons, mostly triangles, at the line intersections. The subtraction of axial lines from urban areas of 70 AI cities has produced 65,692 blocks, of which 41,044 are considered for further analysis after omitting intersectional blocks smaller than 300 m^2, thus preserving the smallest blocks containing buildings found in the historic centers of Chioggia and San Benedetto del Tronto. Due to the relatively small width of the streets on the urban scale, axial blocks match well with urban blocks and can be used as proxies for their shape analysis. They are hereafter referred to as "blocks".

Table 1 (first part): Catalogue of seventy towns and cities along the Adriatic and Ionian coast (listed counterclockwise from Peloponnese to Sicily). Axial map measures of the number of lines N, mean depth $\overline{D}$, and allometric depth D_a; Block shape measures of the number of blocks Q, mean elongation $\overline{RD}$, and mean fragmentation $\overline{DF}$; Length of Δ_{LU} segments between points $(RD:_l, DF:_l)$ and $(RD:_u, DF:_u)$ in the shape configuration matrix (Figure 5).

	Country	Axial			Shape			Matrix
	City	N	$\overline{D}$	D_a	Q	$\overline{RD}$	$\overline{DF}$	Δ_{LU}
	GREECE							
1	Koroni	255	2252.2	0.126	79	1.11	0.062	0.593
2	Methoni	298	2305	-0.054	91	1.11	0.09	0.652
3	Pylos	283	2531.6	0.107	106	1.149	0.054	0.763
4	Zakynthos	488	4401.4	-0.050	269	1.129	0.045	0.766
5	Patras	5362	101712.6	-0.033	2707	1.149	0.086	0.706
6	Aigio	1518	19584.7	-0.036	516	1.159	0.096	0.663
7	Korinthos	269	1832.4	-0.150	421	1.208	0.055	0.841
8	Nafpaktos	667	7386.2	0.061	247	1.146	0.071	0.719
9	Mesolonghi	647	4055.4	-0.499	447	1.095	0.056	0.784
10	Lefkada	597	4158.6	-0.369	301	1.239	0.064	0.734
11	Vonitsa	371	2372.9	-0.311	156	1.111	0.064	0.62
12	Preveza	846	7992.8	-0.170	292	1.212	0.124	0.479
13	Corfu	2619	48950.6	0.170	577	1.258	0.16	0.598
	ALBANIA							
14	Sarandë	1705	41307.8	0.559	351	1.189	0.15	0.494
15	Vlorë	4728	94028.4	0.053	827	1.211	0.219	0.68
16	Durrës	5685	82156.7	-0.322	1291	1.271	0.234	0.684
	MONTENEGRO							
17	Budva	978	11903.1	0.039	264	1.187	0.156	0.551
18	Kotor	377	5512	0.511	70	1.171	0.193	0.616
19	Herceg Novi	1292	31975.4	0.664	187	1.328	0.261	0.474
	CROATIA							
20	Dubrovnik	1495	29129.7	0.381	355	1.258	0.147	0.567
21	Korčula	309	3384.6	0.283	73	1.329	0.193	0.398
22	Hvar	541	7491.8	0.348	137	1.198	0.131	0.434
23	Stari Grad, Hvar	472	6068.2	0.315	123	1.147	0.097	0.674
24	Makarska	622	5242.4	-0.191	190	1.221	0.153	0.589
25	Omiš	107	807.3	0.231	28	1.285	0.132	0.657
26	Split	5924	109566.5	-0.088	1493	1.251	0.167	0.538
27	Šibenik	1221	18150.2	0.172	332	1.251	0.194	0.368
28	Biograd na Moru	811	7790.7	-0.141	215	1.174	0.152	0.659
29	Zadar	3789	67942.2	0.016	876	1.249	0.214	0.678
30	Senj	616	9307.8	0.395	110	1.351	0.215	0.465
31	Rijeka-Kastav	11375	540137.5	0.657	1720	1.286	0.249	0.534
32	Opatija-Volosko	908	18066.6	0.553	135	1.252	0.183	0.398
	Pula	1758	25293.5	0.029	506	1.202	0.154	0.613
34	Rovinj	1018	15763	0.268	221	1.222	0.162	0.481
35	Poreč	708	7141.6	-0.051	207	1.2	0.146	0.564
36	Umag	625	6093.1	-0.047	183	1.21	0.137	0.626

Table 1 (second part)

	SLOVENIA							
37	Piran	316	2907.5	0.102	99	1.128	0.095	0.423
38	Izola	753	7273.9	-0.113	176	1.231	0.195	0.612
39	Koper	1778	26845.8	0.074	515	1.303	0.157	0.6
	ITALY							
40	Muggia	411	5118.9	0.325	67	1.277	0.095	0.573
41	Trieste	6864	185283.4	0.245	1831	1.268	0.195	0.59
42	Monfalcone	2035	25608.7	-0.150	643	1.244	0.157	0.631
43	Grado	286	1924.1	-0.181	202	1.136	0.095	0.605
44	Venice	3201	80084.1	0.400	888	1.216	0.195	0.627
45	Chioggia	2201	28147.1	-0.157	745	1.384	0.157	0.682
46	Cesenatico	794	8632.4	-0.011	382	1.225	0.095	0.761
47	Pesaro	2536	41142.9	0.038	930	1.375	0.195	0.642
48	Fano	1453	13996.5	-0.315	622	1.206	0.157	0.681
49	Ancona	3990	74533.6	0.041	968	1.28	0.095	0.511
50	San Benedetto	946	7908.8	-0.326	494	1.235	0.195	0.701
51	Ortona	454	4631.1	0.095	250	1.141	0.157	0.542
52	Termoli	1468	23603.6	0.194	359	1.245	0.095	0.581
53	Manfredonia	1153	11434.7	-0.216	853	1.132	0.195	0.696
54	Barletta	1122	9968.2	-0.317	579	1.202	0.157	0.658
55	Trani	1851	14217	-0.615	820	1.214	0.095	0.672
56	Molfetta	1057	8193.8	-0.436	909	1.16	0.195	0.753
57	Bari	2677	26757.2	-0.463	1396	1.187	0.157	0.682
58	Monopoli	1461	14243.5	-0.304	622	1.164	0.095	0.723
59	Brindisi	2100	27235.8	-0.129	1028	1.21	0.195	0.602
60	Otranto	494	6639.4	0.345	128	1.237	0.157	0.638
61	Gallipoli	667	7089.6	0.020	330	1.155	0.095	0.695
62	Taranto	324	2086.2	-0.263	89	1.199	0.195	0.675
63	Crotone	722	5409.5	-0.354	387	1.149	0.157	0.573
64	Reggio Calabria	2745	38613.9	-0.129	1098	1.2	0.095	0.729
65	Messina	6242	146458.5	0.134	1980	1.252	0.195	0.645
66	Acireale	2172	30196.5	-0.070	389	1.225	0.157	0.737
67	Catania	9419	212238.8	-0.031	3037	1.318	0.095	0.655
68	Augusta	446	4050.9	-0.016	272	1.213	0.195	0.731
69	Siracusa	2347	33055.4	-0.080	998	1.154	0.157	0.724
70	Avola	1195	7259.2	-0.717	855	1.288	0.095	0.862
	Min	107	807.3	-0.717	28	1.095	0.045	0.368
	Max	11375	540137.5	0.665	3037	1.384	0.261	0.862
	Mean	1842.3	35665.5	0.001	586.3	1.215	0.138	0.627

3   ELONGATION AND FRAGMENTATION OF BLOCK SHAPE

The study employs two measures for the analysis of block shapes, originally developed for the study of building plans (Shpuza and Peponis, 2008), and later applied to the study of urban areas and geographical features (Shpuza, 2011). The measures are based on the spatial relationships among internal locations, which are defined as equally distributed points in a square grid, classifying the representation in the category of internal point indices (Blair and Biss, 1967). Relative Distance (*RD*) is a measure of shape elongation or compactness and is quantified as the aggregate metric shortest-path distances *MD* within a shape relativized by the aggregate of such distances within an equal area square MD_{eas}

$$RD = \frac{MD}{MD_{eas}}$$

$$MD = \sum_{i=1, j=1}^{i=n, j=n-1} md_{ij}$$

where md_{ij} is the metric shortest-path distance between two points i and j made dimensionless by dividing it by the grid dimension, and n is the number of points representing the shape. MD_{eas} is obtained by the function $MD_{eas} = 0.4828\, n^{2.5109}$, which expresses the trendline of the plot between the number of representation points in the square (4, 9, … 3600) and *MD* (13.7, 117.7, … 405,391,392).

Directional Fragmentation (*DF*) measures the degree of fragmentation in a shape and is quantified by the total amount of visual depth among all the points within the shape relativized for the number of points

$$DF = \frac{1}{n(n-1)} \sum_{i=1, j=1}^{i=n, j=n-1} vd_{ij}$$

where vd_{ij} is the visual depth between two points in the shape. The measures *RD* and *DF* are calculated using the Java program *shapeQ*, which was developed for the purpose of this study by building upon the calculation of *metric shortest-path distance* and *visual depth* in *depthmapX* (depthmapX DT, 2017), and where, unlike *depthmapX*, each polygon is represented with a varying number of points depending on its shape complexity. Block shapes in AI sample are represented with an initial count of 250 points and increasing until all bottlenecks are overcome, and full coverage of the area is achieved. The two measures are considered coupled and studied according to the location of data points in the *RD* vs *DF* scatterplot as well as the range of 12 colours based on regions of the plot (Figure 2).

4   THE DISTRIBUTION OF BLOCK ELONGATION AND FRAGMENTATION IN CITIES

Scatterplots between *RD* and *DF* reveal characteristics of block shapes that are linked with both internal forces related to plot size and the ways of plot aggregation, and external forces related to

the topo-geometry of street patterns, which reflect the minimization of travel distances and the intelligibility of navigation in streets. Urban block shapes are the results of three kinds of deformations of the basic elementary square: dissection, which is found in distributory street patterns, stretching, found in bilateral and conjoint patterns, and bending, in serpentine patterns on hilly terrains.
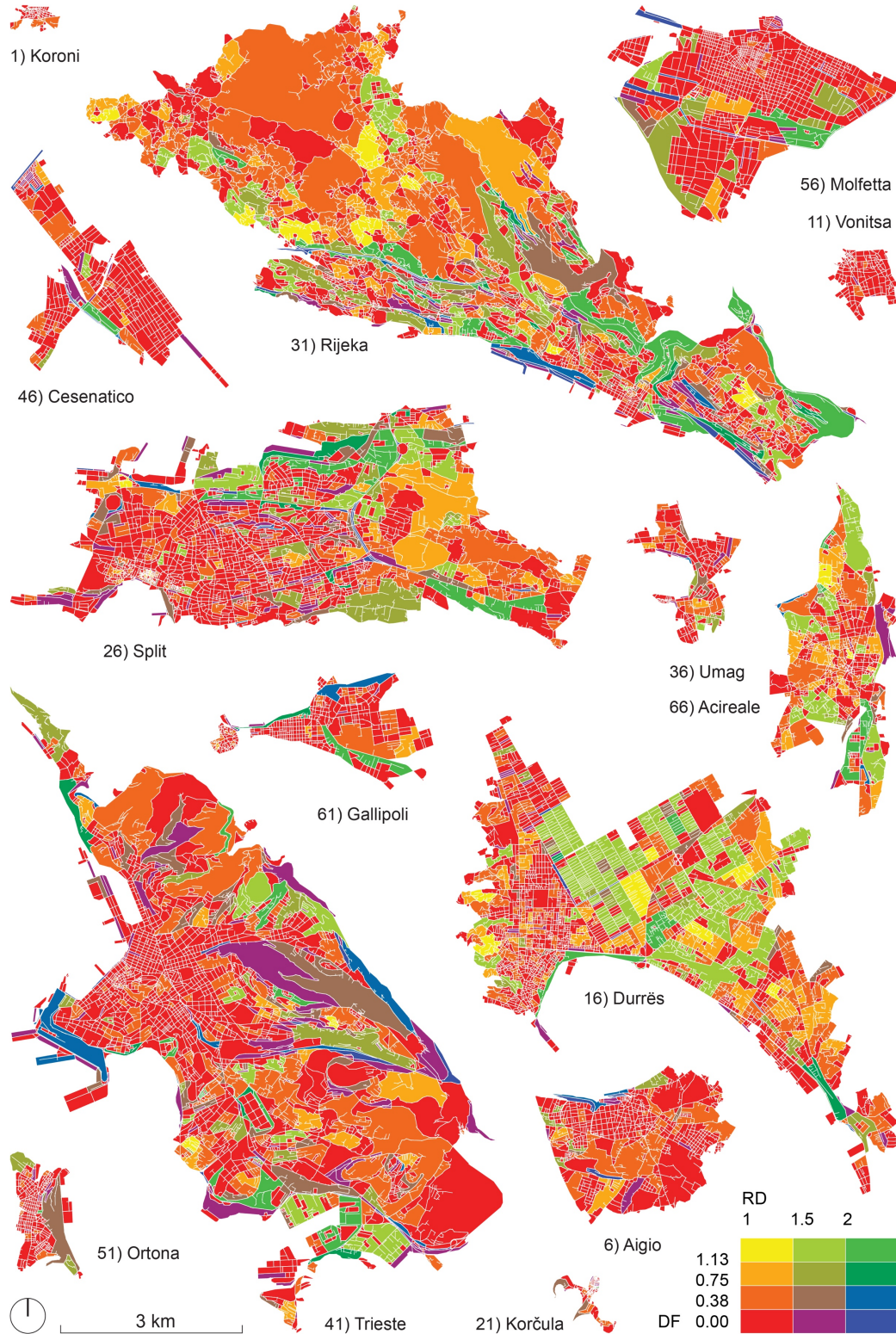

Figure 2: Boundary shapes of blocks of every five cases in the sample of 70 Adriatic and Ionian coastal cities colored according to *RD* and *DF* values as per the legend in the lower right.

Figure 3: Scatterplots between shape elongation *RD* and shape fragmentation *DF* of the blocks in every five cases from the AI sample of coastal cities. The distribution and the density of data points in the scatterplot is scrutinized as a signature of the city's spatial structure.

The distribution of elongation and fragmentation of block shape for each city is investigated by studying the location of data points in the *RD* vs *DF* scatterplots (Figure 3). First, a common feature of all the cases is that most blocks are concentrated in the lower-left corner of the scatters, coinciding with compact and convex blocks. Such concentration gives the scatterplots the structure of a comet with a heavy tip that gradually rarifies towards the top and the right. However, the rarefication is not even, and generally, the comets stretch in two tails. The vertical tail runs along the slope of the limit line including shapes that are both compact and fragmented (low *RD*, high *DF*), representing blocks with internal cul-de-sacs in distributory post-war

developments in the outskirts of the cities. The horizontal tail stretches along the horizontal axis and includes blocks with convex shapes (*DF*=0) that range from squares to elongated rectangles, which are found primarily in gridiron street patterns but also in conjoint street patterns (Marshall, 2005). The zone between the two tails includes shapes that are bent and moderately dissected (low *RD*, low *DF*). However, this zone does not develop far from the tip indicating the limit to the combined action of bending and dissecting in urban blocks. The less the middle zone is developed, the more the tails extend away from the dense triangular tip. The stretching of the scatters in two tails appears as a second common feature across the sample, albeit manifested in various degrees.

Each city exhibits differences in the percentages of blocks belonging to the tails and the magnitude of tails' lengths. In some cases like Koroni and Vonitsa, the tails are short and hardly noticeable, indicating the lack of blocks with dissecting cul-de-sacs and overly elongated blocks. In Durrës and Acireale the vertical tails are more extensive than the horizontal ones, whereas in Aigio and Split, the two tails bend closer to each other compared to other cases in the sample. Cesenatico and Avola exhibit the clearest separation between the two tails, whereas small towns such as Koroni, Vonitsa, and Ortona have shorter tails in comparison to large cities such as Durrës, Rijeka, and Trieste.
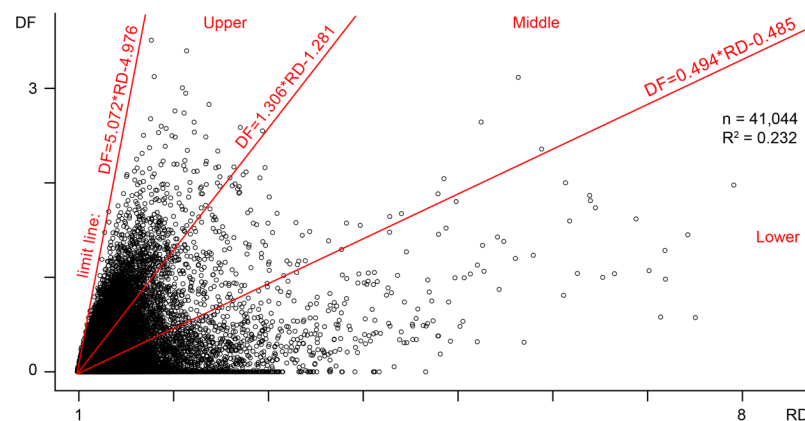

Figure 4: The scatterplot between shape elongation *RD* and fragmentation *DF* for all 41,044 blocks in 70 Adriatic and Ionian coastal cities. The region on the right of the limit line is split into three areas, (Upper, Middle, and Lower), with equal angles at the origin using the equations shown in red.

In lieu of any known statistical measure that captures different distributions of data points in the *RD* vs *DF* scatterplot, I develop a model for quantifying the differences in the two-tail comets with the aim of expressing a quality urban form. First, I investigate the scatterplot of all 41,044 blocks in 70 cities combined (Figure 4). The overall scatter reinforces the earlier readings about the dense tip and the elongation of scatters in two tails. As a mathematical necessity of the link between *RD* and *DF*, i.e., it is not possible to increase shape dissection without also increasing its elongation, there exist an empty triangular region along the *DF* axis. While the theoretical boundary of this zone is yet to be defined, the line (or curve) should fall to the left of the limit line (*DF* = 5.072* *RD* – 4.976), which is discovered empirically by connecting the lower left extremity corner occupied by the circle (*RD*=0.981, *DF*=0) with the most fragmented and

compact shape in the sample (RD=1.273, DF=1.475) located at the left extremity of the scatterplot. To gauge the extent and density of each tail, I divide the RD vs DF plot to the right of the limit into three sectors Upper (U), Middle (M), and Lower (L), by splitting the angle at the scatterplot origin into three equal parts (Figure 4). The upper sector U includes 16.15% of the total number of 41,044 blocks in the AI sample, the M sector includes 18.37% of the blocks, and the L sector includes 65.48% of the blocks.

For each city, I scrutinize the distribution of data points in the three sectors defined above. For the L sector, I count the number of data points within the sector Q_l, the sum of elongation values of the data points falling within the sector $\sum rd_l$, and the sum of fragmentation values within the sector $\sum df_l$. These values are then relativized by comparing them to all the blocks in the city: according to the percentage of points in the sector $Q{:}_l = Q_l/Q$, the share of elongation in the sector $RD{:}_l = \sum rd_l/(Q * \overline{RD})$, and the share of fragmentation in this sector compared to all city blocks $DF{:}_l = \sum df_l/(Q * \overline{DF})$. Likewise, for the other two sectors M and U, I calculate ($Q{:}_m$, $RD{:}_m$, $DF{:}_m$) and ($Q{:}_u$, $RD{:}_u$, $DF{:}_u$). The symbol ":" denotes a ratio, while the subscripts "l, m, and u" denote the shape sector (Table 1). By definition, $RD{:}_l + RD{:}_m + RD{:}_u = 1$, and $DF{:}_l + DF{:}_m + DF{:}_u = 1$. The ratios are affected by the percentage of data points in each sector as well as the location of the points in each sector, e.g., a high $DF{:}_l$ ratio indicates a large share of points in the L sector and/ or high DF values compared to the rest of the city.

5   SHAPE CONFIGURATION MATRIX

Street networks in each city are represented with axial maps and analysed using *depthmapX* (depthmapX DT, 2017; Turner, 2010). For each city, I record the number of axial lines N, the total topological depth ($D = \overline{D} * N$), and connectivity ($C = \overline{C} * N$). I calculate the allometric depth D_a for each city using the residuals to the linear regression in the lnN vs lnD plot (Shpuza, 2017).

$$D_a = lnD - ln(1.453N^{2.301})$$

Similarly, the allometric connectivity C_a is calculated as

$$C_a = lnC - ln(4.726N^{0.945})$$

Allometric depth is correlated to the mean *Integration HH* (Hillier and Hanson, 1984) with (R^2 = -0.659) reported for the AI sample (Shpuza, 2017). Low values of D_a indicate high integration for the street network in a city. For brevity, hereafter, allometric depth is referred to as "integration"

I carry out several correlation tests on the link between block shape and street network integration, but I discuss only two that show notable correlations. The percentage of convex blocks in a city (DF < 0.02) has a considerable affinity with integration ($Q{:}_{DF<0.02}$ vs D_a, R^2 = -0.311), where the threshold DF=0.02 is used to account for the effect of axial stubs in the convex blocks. In other words, the higher the percentage of convex blocks the higher the integration. Considering each scatterplot sector separately, mean values of elongation $\overline{RD}_l$, $\overline{RD}_m$, and $\overline{RD}_u$, and mean fragmentation $\overline{DF}_m$, and $\overline{DF}_u$ show weak correlations with the integration. In contrast,

the fragmentation of the L sector $\overline{DF_l}$ shows the highest correlation with D_a at (R^2 = -0.309). To be noted is the fact that the fragmentation of the horizontal tail $\overline{DF_l}$ is heavily influenced by the percentage of convex blocks in the city $Q_{DF<0.02}$ as discussed earlier.

I test whether the distribution of elongation and fragmentation considered for all three sectors together rather than separately has a better affinity to the street network integration than the percentage of the convex blocks in the city. From this perspective, the distribution of shape elongation and fragmentation is configurational since the measures in each sector are compared to all other sectors. I superimpose the *RD:* and *DF:* ratios for three sectors L, M and U in a scatterplot between *RD:* and *DF:* ratios, which I term shape configuration matrix. In the matrix, each city is represented with three data points L: (x= *RD:l:*, y= *DF:l*), M:, and U: representing the ratios in three sectors L, M and U (Figure 5).
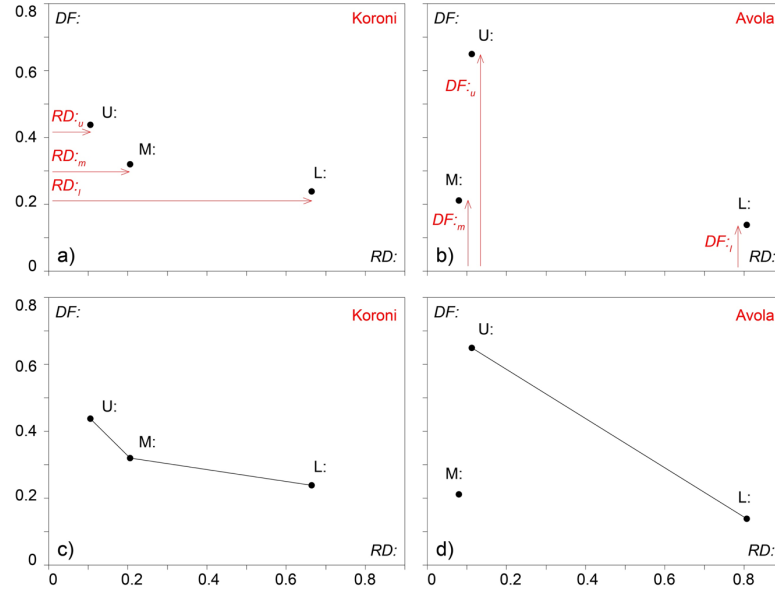

Figure 5: The urban block shape configuration matrix defined as the scatterplot between elongation ratios *RD:* and fragmentation ratios *DF:* with the values of three sectors L, M and U superimposed. a) *RD:* values in L, M and U sectors in the town of Koroni, b) *DF:* values in L, M and U sectors in Avola, c) The two-segment representation of Koroni produced by connecting L, M and U points, d) The Δ_{LU} segment representation of Avola produced by connecting (*RD:l*, *DF:l*) and (*RD:u*, *DF:u*) points.

Neither distances Δ_{LM} between L: and M:, and Δ_{MU} between M: and U: in the shape configuration matrix, nor their sum $\Delta_{LM}+\Delta_{MU}$ (Figure 5(c)), show any significant relationship to integration as shown by weak correlations with D_a. Let us now disregard the M: points and consider the length of the segments Δ_{LU} between points L: (*RD:l*, *DF:l*) and U: (*RD:u*, *DF:u*), (Figure 5(d)), which is measured as

$$\Delta_{LU}= \sqrt[2]{(RD:_u - RD:_l)^2 + (DF:_u - DF:_l)^2}$$

The segments Δ_{LU} for 70 cities in AI sample are illustrated grouped in six ranges according to their length (Figure 6). There exists a correspondence between the length of Δ_{LU} segments and the relative location of the ratios in the *RD:* vs *DF:* matrix. The shortest segments in the range (0.368 ~ 0.511) connect two narrow regions within the overall convex hulls of datapoints L: and U:,

which are placed quite symmetrically at the inner sides of the larger hulls (Figure 6(a)). As the ranges increase (Figure 6(b) – (f)), the regions become larger and occupy areas from the center of the overall hulls to their outer sides, maintaining an overall symmetry. While short Δ_{LU} segments between L: and U: points have similar slopes, the longer segments exhibit a greater variety of slopes indicating a greater range of combinations of L: and U: values in these cities. In general, the short Δ_{LU} segments are found in cities built on sloped terrains such as Šibenik, Korčula, and Opatija mainly on the Balkan coast, whereas long segments coincide with cities with substantial areas covered by gridiron street patterns such Avola, Korinthos, Mesolonghi, and Zakynthos.
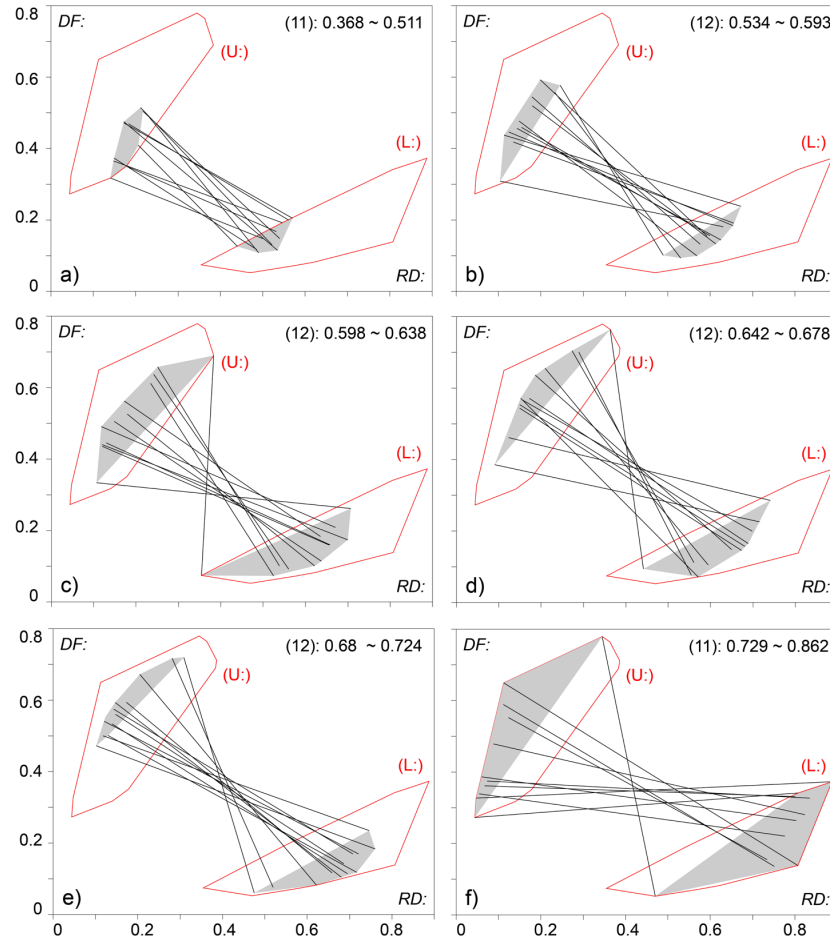

Figure 6: Segments Δ_{LU} (black lines) drawn between ($RD{:}_l$, $DF{:}_l$) and ($RD{:}_u$, $DF{:}_u$) points plotted in the shape configuration matrix for 70 AI towns and cities, and split into six groups of 11 or 12 cities according to their diagonal lengths from the 11 shortest (a) to the 11 longest (f). The convex hulls enclosing the datapoints for the entire AI sample are marked with red polygons (L:) and (U:), and the convex hulls enclosing datapoints belonging to each range are marked with solid grey polygons.

6   RELATIONSHIP BETWEEN SHAPE CONFIGURATION AND STREET NETWORK INTEGRATION

The value of Δ_{LU} shows the strongest affinity so far with integration (R^2=-0.352) (Figure 7(a)), which, like all other correlations presented here, has a high significance at (p<0.0001). As is commonly known in space syntax studies, the local descriptor of axial connectivity is a good

predictor of global integration: (C_a vs D_a, R^2 = -0.504) for the case of AI cities. I ask whether the block shape configuration, another local measure, can be complementary to connectivity in giving a better affinity with integration. Since C_a has, by definition, a mean of 0 for AI sample, I relativize Δ_{LU} towards its mean 0.627 for AI sample in order to enable their summation

$$rel\Delta_{LU} = \frac{\Delta_{LU} - 0.627}{0.627}$$

It should be noted that the relativized measures maintain the same correlations with the integration as original measures. The sum $\alpha*rel\Delta_{LU}+C_a$ (α=0.4) shows a correlation (R^2 = -0.573) with D_a (Figure 7(b)), indicating that the two local measures explain integration better coupled than considered separately.
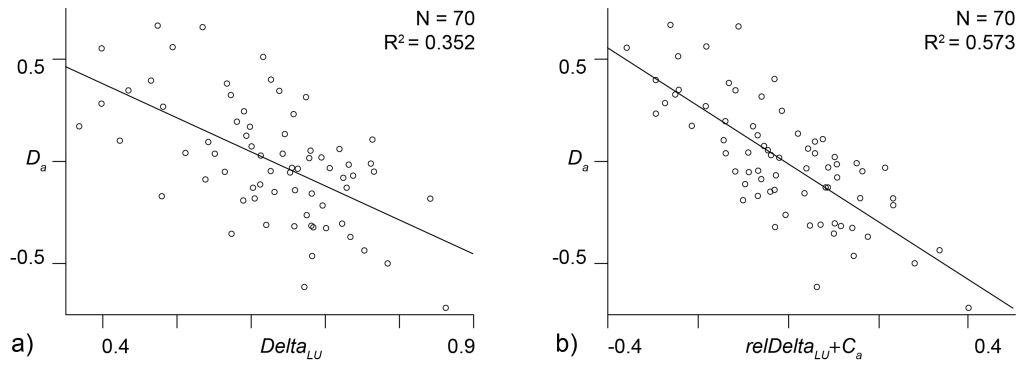

Figure 7: Correlations between shape configuration measures and street network integration for 70 AI coastal cities. a) Length of segment Δ_{LU}, drawn between ($RD:_l$, $DF:_l$) and ($RD:_u$, $DF:_u$), vs. allometric depth D_a; b) Sum of relativized $rel\Delta_{LU}$ and relativized axial connectivity relC vs. allometric depth D_a.

Generally, long Δ_{LU} segments, which are correlated with high integration, connect points within an area of the (L) region that is roughly defined by (RD: 0.5~0.85, DF: 0.1~0.4), to points within an area of the (U) region about (RD: 0.1~0.3, DF: 0.3~0.8) Figures (6(e) and 6(f)). Accordingly, the findings are translated into normative guidelines about how to increase the global integration of street networks through the local scale design of the background streets and urban block shapes. First, increase the number of blocks that are both elongated and convex (medium RD, low DF) and/or increase the elongation of convex blocks (medium RD). In other words, rectangular blocks in gridiron street patterns coincide with higher integration than square blocks. As discussed earlier, increasing the number of convex blocks alone ($Q_{DF<0.02}$) will not have the same effect as the combined increase of elongation. Further work is needed to understand the combined effect of the number of blocks and fragmentation on the DF: ratio since the two have an opposite effect. For example, a higher DF: ratio is caused both due to more blocks within the L sector as well as a higher DF values of the blocks, i.e., increased fragmentation usually due to shape bending.

Second, reduce the number of fragmented blocks with internal dissections and/or reduce the elongation of internally dissected blocks (low RD), which is achieved by preferring dissected

blocks with convex outer shapes to those with bent outer shapes, and dissected blocks that have compact outer shapes rather than elongated outer shapes.

Another relationship of interest is the one between the percentage of points in the M sector $Q_{:m}$ vs Δ_{LU} ($R^2 = -0.809$), i.e., the more points fall in either L or U sectors, the longer the Δ_{LU} distances thus the higher the integration. Shapes that fall in the M sector are characterized by overall shape bending, and in practical terms, reducing the overall bending of urban block shape would increase the Δ_{LU} values. However, as discussed in the previous section, the number of points in the M sector itself does not correlate well with integration ($Q_{:m}$ vs D_a, $R^2 = -0.233$), and further work is needed to understand their mutual coeffects. Third, reduce the overall bending of urban blocks, such as those typically found in serpentine street patterns in hilly terrains, to increase street network integration. It should be noted that, given the configurational structure of the matrix, the guidelines work best if considered combined.

Fourth, contrary to what might appear as obvious, increasing the number of convex blocks in the city does not necessarily increase integration. The correlation of $relQ_{DF<0.02}+C_a$ vs D_a at ($R^2=-0.413$) shows that the combined effect of the percentage of convex blocks in the city and street connectivity is a weaker prediction of integration than the combined effect of Δ_{LU} and street connectivity ($R^2 = -0.573$) discussed above.

7   CONCLUSIONS

The study developed a method of quantifying the distribution of elongation and fragmentation of block shape in cities based on the scatterplot between the measures *RD* and *DF*. To analyse block shapes, the Java program *shapeQ* is developed by building on the calculation of *metric shortest distance* and *visual distance* in *depthmapX*, where each shape is flooded with different tessellation sizes depending on shape complexity. Block shapes in cities reveal two common features of distribution of elongation and fragmentation in the *RD* vs *DF* plot: First, a high percentage of blocks are compact and convex; Second) the rest of the blocks show two behaviours materialized as two tails in the scatterplots: either increased elongation while maintaining convexity or minimal dissection or increased dissection through internal cul-de-sacs and tree-like streets while restricting elongation. The combined bending and elongation are infrequent resulting in a sparser diagonal in the scatterplot. Three sectors in the scatterplots are proposed in order to quantify the stretching of the two tails in the scatterplots. However, while the percentages of points and the amount of elongation and fragmentation in each sector is not related to the street network global integration, the combined ratios in the two sectors, which coincide with the two tails, indicate a considerable and significant link with the integration. The ratios interface is discussed as a shape configuration matrix that enables the comparison of shape features in a sector to all the other sectors. The ratios are complementary to the local axial connectivity since both show an increased correlation with integration compared to each one separately. In conclusion, the shape configuration matrix, which is used to define the spatial

signature of a city based on block shape, supports comparative urban studies, while it opens the way for further research on the link between geometric and topological characteristics of street networks.

Acknowledgment

REFERENCES

Blair, D.J., and Biss, T.A. (1967) "Measurement of shape in geography: An appraisal of methods and techniques", *Bulletin of Quantitative Data for Geographers 11*, Nottingham: Nottingham University, Department of Geography.

depthmapX Development Team (2017) depthmapX (Version 0.6.0) [Computer software] https://github.com/SpaceGroupUCL/depthmapX/

Figueiredo, L. and Amorim, L. (2005) "Continuity lines in the axial system" *The Fifth Space Syntax International Symposium* (Delft University of Technology).

Hillier, B. (1989) "The architecture of the urban object" *Ekistics, Special Issue on Space Syntax Research* 56(334/335): 5–21.

Hillier, B. (1999) "The hidden geometry of deformed grids: Or, why space syntax works when it looks as though it shouldn't" *Environment and Planning B: Planning and Design* 26: 169-191.

Hillier, B. and Hanson, J. (1984) *The Social Logic of Space*. Cambridge: Cambridge University Press.

Hillier, B., Penn, A., Hanson, J., Grajewski, T. and Xu, J. (1993) "Natural movement: Or configuration and attraction in urban pedestrian movement" *Environment and Planning B: Planning and Design* 20: 29–66

Hillier, B., Turner, A., Yang, T. and Park, H. (2010) "Metric and topo-geometric properties of urban street networks: Some convergencies, divergencies and new results" *Journal of Space Syntax*, 1(2): 258-279.

Louf, R. and Barthelemy, M. (2014) "A typology of street patterns" *Journal of The Royal Society Interface* 11(101): 20140924.

Marshall, S. (2005) *Streets and Patterns*. London: Spon.

Peponis, J., Bafna, S. and Zhang, Z. (2008) "The connectivity of streets: Reach and directional distance" *Environment and Planning B: Planning and Design* (35)5: 881-901.

Serra, M. and Hillier, B. (2019) "Angular and metric distance in road network analysis: A nationwide correlation study" *Computers, Environment and Urban Systems*, 74, 194-207.

Shpuza, E. (2011) "A coupled configurational description of boundary shape based on distance and directionality" *Artificial Intelligence for Engineering Design, Analysis and Manufacturing* 25: 357–374.

Shpuza, E. (2013) "Foreground networks during urban evolution: The effect of length and connectivity on street network integration", *Proceedings of the Ninth International Space Syntax Symposium* (Sejong University).

Shpuza, E. (2014) "Allometry in the syntax of street networks: Evolution of Adriatic and Ionian coastal cities 1800–2010" *Environment and Planning B: Planning and Design* 41(3): 450–471.

Shpuza, E. (2017) "Relative size measures of urban form based on allometric subtraction" *Environment and Planning B: Urban Analytics and City Science* 44(1), 141-159.

Shpuza, E. and Peponis, J. (2008) "The effect of floorplate shape upon office layout integration" *Environment and Planning B: Planning and Design* 35(2): 318–336.

Southworth, M. and Owens, P. (1993) "The evolving metropolis: Studies of community, neighborhood and street form at the urban edge" *Journal of the American Planning Association* 59(3): 271–287.

Turner, A. (2001) "Angular analysis" *Proceedings of the Third international Symposium on Space Syntax*, 30-11 (Georgia Institute of Technology).

Turner, A. (2010) UCL Depthmap: Spatial Network Analysis Software (University College London).